

ARTICLE OPEN



Phenotypically-defined stages of leukemia arrest predict main driver mutations subgroups, and outcome in acute myeloid leukemia

François Vergez^{1,2,3,4}, Laetitia Largeaud^{1,2,3}, Sarah Bertoli^{3,5}, Marie-Laure Nicolau¹, Jean-Baptiste Rieu¹, Inès Vergnolle¹, Estelle Saland³, Audrey Sarry⁵, Suzanne Tavitian⁵, Françoise Huguet⁵, Muriel Picard⁵, Jean-Philippe Vial⁶, Nicolas Lechevalier⁶, Audrey Bidet⁶, Pierre-Yves Dumas⁷, Arnaud Pigneux⁷, Isabelle Luquet¹, Véronique Mansat-De Mas¹, Eric Delabesse¹, Martin Carroll⁴, Gwenn Danet-Desnoyers⁴, Jean-Emmanuel Sarry^{3,8} and Christian Récher^{2,3,5}

© The Author(s) 2022

Classifications of acute myeloid leukemia (AML) patients rely on morphologic, cytogenetic, and molecular features. Here we have established a novel flow cytometry-based immunophenotypic stratification showing that AML blasts are blocked at specific stages of differentiation where features of normal myelopoiesis are preserved. Six stages of leukemia differentiation-arrest categories based on CD34, CD117, CD13, CD33, MPO, and HLA-DR expression were identified in two independent cohorts of 2087 and 1209 AML patients. Hematopoietic stem cell/multipotent progenitor-like AMLs display low proliferation rate, *inv(3)* or *RUNX1* mutations, and high leukemic stem cell frequency as well as poor outcome, whereas granulocyte-monocyte progenitor-like AMLs have *CEBPA* mutations, *RUNX1-RUNX1T1* or *CBFB-MYH11* translocations, lower leukemic stem cell frequency, higher chemosensitivity, and better outcome. *NPM1* mutations correlate with most mature stages of leukemia arrest together with *TET2* or *IDH* mutations in granulocyte progenitors-like AML or with *DNMT3A* mutations in monocyte progenitors-like AML. Overall, we demonstrate that AML is arrested at specific stages of myeloid differentiation (SLA classification) that significantly correlate with AML genetic lesions, clinical presentation, stem cell properties, chemosensitivity, response to therapy, and outcome.

Blood Cancer Journal (2022)12:117; <https://doi.org/10.1038/s41408-022-00712-7>

INTRODUCTION

Normal blood cell maturation is organized according to a functional hierarchy at the top of which are multipotent hematopoietic stem cells (HSC). Immunophenotypically, human HSCs are enriched in a population of Lin⁻, CD34⁺, CD38⁻, CD90⁺, and CD45RA⁻ cells [1–4]. Upon differentiation, HSC gives rise to multipotent progenitors (MPP), which retain the ability to produce all blood lineages but have lost their self-renewal capacity [4]. The classical model of hematopoiesis [5, 6] postulates that MPPs are then orientated toward either the lymphoid or myeloid lineage, developing into common myeloid progenitors (CMP) or lymphoid-primed multipotent progenitors (LMPP) which can still produce defined myeloid cell types. Along the myeloid pathway, CMP can differentiate into either granulocyte-monocyte progenitors (GMP) or megakaryocyte-erythroid progenitors (MEP). GMPs finally differentiate into granulocyte progenitors (GP) or monocyte progenitors (MP).

Acute myeloid leukemia (AML), the neoplastic counterpart of early hematopoiesis, is caused by the excessive proliferation of

transformed hematopoietic progenitors which show great heterogeneity at the morphological, immunophenotypic, cytogenetic, and molecular levels [7]. Recent studies have shown that leukemic clones might develop from pre-leukemic hematopoietic cells carrying mutations in genes such as *DNMT3A*, *TET2*, or *ASXL1*, which then accumulate a series of secondary mutations some of which will block differentiation while others induce uncontrolled proliferation [8, 9]. Importantly, AML is initiated and maintained by rare and immunophenotypically diverse leukemic stem cells (LSC), phenocopying the hierarchical organization of normal hematopoiesis [10–12].

Despite a better characterization of AML and higher efficacy of new AML therapies, biomarkers for response prediction are currently lacking, in part because genomic aberrations have shown only limited predictive value [13]. More accurate response predictions, which go beyond genomics, are needed for some of the newest approaches to AML treatment.

The proteome and the surfaceome have been considered a promising and complementary fields to the genome for

¹Laboratoire d'Hématologie, Centre Hospitalier Universitaire de Toulouse Oncopole, Toulouse, France. ²Université Toulouse III Paul Sabatier, Toulouse, France. ³Cancer Research Center of Toulouse, UMR1037 INSERM, ERL5294 CNRS, Toulouse, France. ⁴Stem Cell and Xenograft Core, University of Pennsylvania, Perelman School of Medicine, Philadelphia, PA, USA. ⁵Service d'Hématologie, Centre Hospitalier Universitaire de Toulouse, Institut Universitaire du Cancer de Toulouse Oncopole, Toulouse, France. ⁶Laboratoire d'Hématologie, Centre Hospitalier Universitaire de Bordeaux, Pessac, France. ⁷Service d'Hématologie Clinique et de Thérapie Cellulaire, Centre Hospitalier Universitaire de Bordeaux, Pessac, France. ⁸Centre Hospitalier Universitaire de Toulouse, Institut Universitaire du Cancer de Toulouse Oncopole, Toulouse, France. ✉email: Vergez.Francois@iuct-oncopole.fr; Recher.Christian@iuct-oncopole.fr

Received: 22 February 2022 Revised: 22 July 2022 Accepted: 26 July 2022

Published online: 16 August 2022

elucidating cancer biology and identifying diagnostic and predictive biomarkers [14, 15]. However, there are still very few clinically relevant biomarkers and disease subtypes that have been identified by these approaches [16–18].

Here, we did a phenotypic, cytogenetic, and molecular correlative analysis of a very large cohort of AML patients to capture the AML surfaceome that appears to be caused by the stage of leukemia arrest (SLA) and by specific genomic features. We hypothesized that our approach may add to current AML classifications by identifying relevant phenotypic AML subtypes with specific clinical and molecular features as well as information on outcomes after standard treatment. Overall, we anticipated that phenotypic classification associated with the morphological analysis, available within 24 h on the day of diagnosis, could be very useful to begin planning therapeutic strategy in daily practice.

PATIENTS AND METHODS

Patients and samples

Between January 1, 2000 and December 31, 2019, 2448 AML patients (>15 years) were included in the AML database of Toulouse University Hospital (TUH) and 1700 AML patients in the AML database of Bordeaux University Hospital (BUH). Immunophenotyping at diagnosis was available for 2087 TUH patients (median age: 63 years) of which 1266 received intensive chemotherapy [19, 20] (Table 1) and 1209 BUH patients (Table S1). AML patient samples were stored after informed consent at the HIMIP collection (BB-0033-00060). According to French law, HIMIP collections have been declared to the Ministry of Higher Education and Research (DC 2008-307 collection 1) and obtained a transfer agreement (AC 2008-129) after approbation by the “Comité de Protection des Personnes Sud-Ouest et Outremer II” (Ethical Committee). BUH and TUH cohorts are both registered in the Toulouse-Bordeaux DATAML registry [21, 22].

Immunophenotyping

Multi-parameter flow cytometry (MFC) was performed on whole bone marrow (BM) or blood specimens using a standard stain-lyse-wash procedure with ammonium chloride lysis. 1×10^5 cells were stained per analysis tube, and data were acquired on at least 1×10^4 blasts when specimen quality permitted. Data on standardized 8- to 10-color staining combinations were acquired on FACSCanto II cytometers using FACSDiva software (BD Biosciences) or Navios instruments analyzed using Kaluza (Beckman-Coulter). Several different tube configurations were used through the course of the study, all with staining for CD13, CD33, CD34, CD45, CD117, HLA-DR, and cytoplasmic MPO. A blast gate including CD45 dim mononuclear cells was analyzed according to cytomorphologic data.

Next-generation sequencing

DNA samples from 409 AML patients have been obtained after informed consent and stored at the HIMIP collection (BB-0033-00060). Briefly, genomic DNA was extracted from the baseline bone marrow sample using a Qiagen DNA extraction kit (Qiagen). The presence of *FLT3*-ITD was tested as described [19]. Electrophoregram peaks were quantified using GeneMarker 2.2 (SoftGenetics, State College, PA, USA). *CEBPA* screening was performed by classical Sanger sequencing [23]. An extended DNA resequencing was performed using a Illumina NextSeq500 and Sureselect (Agilent, Santa Clara, CA, USA) targeted on the complete coding regions of 46 genes commonly mutated in myeloid malignancies: *ASXL1* (NM_015338.6), *ASXL2* (NM_018263.6), *BCOR* (NM_001123383.1), *BCORL1* (NM_021946.5), *CBL* (NM_005188.4), *CCND2* (NM_001759.4), *CEBPA* (NM_004364.5), *CSF3R* (NM_156039.3), *DHX15* (NM_001358.3), *DNMT3A* (NM_022552.5), *EP300* (NM_001429.4), *ETV6* (NM_001987.5), *EZH2* (NM_004456.5), *FLT3* (NM_004119.3), *GATA1* (NM_002049.4), *GATA2* (NM_032638.5), *IDH1* (NM_005896.4), *IDH2* (NM_002168.4), *JAK2* (NM_004972.4), *KDMSA* (NM_001042603.3), *KDM6A* (NM_021140.4), *KIT* (NM_000222.3), *KMT2D* (NM_003482.4), *KRAS* (NM_004985.5), *MGA* (NM_001164273.2), *MYC* (NM_002467.6), *NF1* (NM_000267.3), *NPM1* (NM_002520.7), *NRAS* (NM_002524.5), *PHF6* (NM_032458.3), *PIGA* (NM_002641.4), *PTPN11* (NM_002834.5), *RAD21* (NM_006265.3), *RUNX1* (NM_001754.5), *SETBP1* (NM_015559.3), *SF3B1* (NM_012433.4), *SMC1A* (NM_006306.4), *SMC3* (NM_005445.4), *SRSF2* (NM_003016.4), *STAG2* (NM_001042749.2), *TET2* (NM_001127208.3), *TP53* (NM_000546.6), *U2AF1* (NM_006758.3), *WT1* (NM_024426.6), *ZBTB7A* (NM_015898.4), *ZRSR2*

(NM_005089.4). Data were processed through two algorithms from GATK (<https://software.broadinstitute.org/gatk>), HaplotypeCaller, and Mutect2, and also through Agilent Surecall software, with a sensitivity of 1% [24, 25]. All variants called by two variant callers were checked using IGV software. Identified variants were curated manually and named according to the rules of the Human Genome Variation Society (hgvs.org).

Bioinformatics analyses

Freely available gene expression datasets for normal hematopoietic stem and progenitor cells GEO:GSE42414 [26], Array Express:E-TABM-978 [12], GEO:GSE74246 [27], GEO:GSE63270 [28] were used for this study.

Statistical analysis

Complete response and relapse rates were defined according to the Cheson criteria [29]. Comparisons were performed using a Mann–Whitney test or Kruskal–Wallis test for continuous variables and Fisher’s exact test for categorical variables with GraphPad Prism. Statistical test results are graphically expressed: * $p < 0.05$, ** $p < 0.01$, *** $p < 0.001$.

Disease-free survival was measured from the date of complete remission until the date of relapse or death. The cumulative incidence of relapse was measured from the date of complete remission until the date of relapse, with death regarded as a competitive event. Overall survival was measured from the date of diagnosis until death. Patients in complete remission were censored at the time of the last contact. The risk groups for prognosis were evaluated for overall and disease-free survival by univariate analysis (log-rank test) using a multivariate model of Cox regression and for the cumulative incidence of relapse by the Fine and Gray test. All calculations were performed using STATA version 13 software (STATA Corp., College Station, TX, USA), all graphs were done using Graph Pad Prism.

More details are provided in Supplemental Information.

RESULTS

Hematopoietic stem and progenitor cells (HSPC)

Immunophenotypes define AML specimens at different stages of the human hematopoietic hierarchy

To define a surrogate phenotype for each stage of normal myeloid maturation, we need to assess by flow cytometry, the expression of markers used to characterize AML routinely on HSPCs. HSC, MPP, CMP, GMP, and GP/MP can be characterized by gating in the lineage negative cell population according to their expression of CD34, CD38, CD90, and CD45RA (Supplemental Fig. 1A, B). Unfortunately, the expression of those markers is not classically evaluated in AML. To overcome this issue, we evaluated the expression levels of four myeloid antigens (CD13, CD33, CD117, and myeloperoxidase [MPO]) as well as CD34 and HLA-DR in 10 normal human bone marrow samples. HSC and MPP were characterized by the absence of MPO expression (Fig. 1A and Supplemental Fig. 1C). The expression of specific myeloid markers such as CD13 or CD33 was detectable from the MPP stage onward. GMP displayed the highest MPO expression (>70% of cells). HLA-DR expression discriminated MP (HLA-DR positive) and GP (HLA-DR negative). These data show that six markers (i.e. CD34, CD117, CD13, CD33, MPO, and HLA-DR) used to diagnose AML in routine clinical practice are differentially expressed in six immunophenotypically defined stages of normal myelopoiesis.

To correlate each stage of normal hematopoiesis with that of individual AML, we transformed HSPC immunophenotypes into immunophenotypic AML signatures (Fig. 1A). Thus, the SLA was assigned to each sample, based on leukemic bulk phenotype, because in the hierarchy of leukemic cells, the majority are stopped in their differentiation pathway. We tested our six-marker immunophenotypic signature by looking at the principal component analysis distribution of 945 AML, extensively characterized by the expression of 16 antigens (Fig. 1B and Supplemental Fig. 2A and B). Our six-marker signature was sufficient to discriminate between different hematopoietic/leukemic groups (Supplemental Fig. 2C, D). Overall, we defined, by flow cytometry, the stage at which the leukemic cell population accumulated as the stage of leukemia differentiation arrest.

Table 1. Characteristics of patients from the TUH cohort.

2087 patients	TUH cohort	HSC-L	MPP-L	CMP-L	GMP-L	GP-L	MP-L
<i>Patients</i>							
Age (median and IQR, years)	65 (54–75)	61 (40–78)	69 (60–78)	69 (58–77)	62 (44–73)	69 (58–75)	63 (51–72)
<60 yr (%)	692 (33.2)	7 (38.9)	112 (24.5)	174 (27.6)	162 (45.0)	34 (28.6)	203 (40.4)
≥60 yr (%)	1395 (66.8)	11 (61.1)	346 (75.5)	456 (72.4)	198 (55.0)	85 (71.4)	299 (59.6)
<i>AML status</i>							
De novo	1423 (70.2)	13 (72.2)	243 (53.1)	400 (63.5)	276 (76.7)	96 (80.7)	395 (78.7)
Secondary to MDS	247 (12.2)	4 (22.2)	75 (16.4)	103 (16.3)	24 (6.7)	5 (4.2)	36 (7.2)
Secondary to MPN	142 (7.0)	1 (5.6)	70 (15.3)	51 (8.1)	12 (3.3)	3 (2.5)	5 (1.0)
Therapy-related	245 (12.1)	0 (0.0)	62 (13.5)	73 (11.6)	43 (11.9)	12 (10.1)	55 (11.0)
Unknown	30 (1.5)	0 (0.0)	8 (1.7)	3 (0.5)	5 (1.4)	3 (2.5)	11 (2.2)
<i>Extramedullary disease</i>							
Liver	100/1603	4/10	22/326	18/484	19/295	5/93	32/395
Spleen	161/1603	3/10	45/326	44/484	23/295	6/93	40/395
Lymph nodes	174/1603	4/10	26/326	37/484	32/295	10/93	65/395
Gingiva	148/1603	0/10	11/326	30/484	23/295	10/93	74/395
Skin	56/1603	3/10	3/326	14/484	10/295	1/93	25/395
<i>Complete Blood Count (median and IQR)</i>							
Hemoglobin (g/L)	9.3 (8.2–10.7)	8.9 (8.3–11.1)	9.0 (8.0–10.2)	9.3 (8.2–10.8)	9.4 (8.3–10.9)	9.4 (8.2–11.1)	9.6 (8.3–10.9)
Platelet count (g/L)	62 (33–112)	75 (37–163)	62 (29–120)	64 (31–115)	56 (32–101)	62 (34–98)	63 (39–110)
WBC count (g/L)	8.01 (2.40–36.79)	3.90 (1.40–12.76)	5.08 (2.05–20.20)	3.60 (1.80–15.53)	8.68 (2.88–44.98)	15.34 (6.9–80.10)	24.72 (4.30–71.36)
<i>Bone marrow evaluation</i>							
Blasts (median and IQR, %)	52 (30–77)	63 (39–90)	44 (29–69)	36 (24–61)	59 (37–76)	86 (62–93)	69 (44–86)
Cytological dysmyelopoiesis	912/1898	5/16	219/401	369/583	131/337	23/99	165/462
<i>Cytogenetic risk</i>							
Favorable (%)	139 (6.9)	0 (0.0)	0 (0.0)	15 (2.4)	119 (33.7)	1 (0.9)	4 (0.8)
Intermediate (%)	1258 (62.0)	9 (50.0)	221 (50.7)	343 (55.7)	165 (46.7)	103 (91.1)	417 (84.8)
Adverse (%)	631 (31.1)	9 (50.0)	215 (49.3)	258 (41.9)	69 (19.5)	9 (8.0)	71 (14.4)
<i>Mutation status (mutated/tested)</i>							
CEBPA mono or bi-allelic	69/865	0/6	1/163	9/248	41/125	4/59	14/264
DNMT3A (exon 23)	130/884	0/8	13/163	32/250	8/155	6/58	71/250
FLT3-ITD	295/1456	5/13	40/264	61/399	28/258	35/94	126/428
FLT3-TKD	57/818	1/6	8/159	15/234	8/152	4/55	21/212
IDH1	101/1120	0/8	10/231	29/325	12/193	13/72	37/291
IDH2	134/1120	1/8	25/231	45/325	23/193	17/72	23/291
NPM1	427/1421	0/9	16/271	49/394	18/232	75/94	269/421
<i>Treatment</i>							
Intensive chemotherapy (%)	1266 (60.7)	12 (66.7)	192 (41.9)	325 (51.6)	269 (74.7)	88 (73.9)	380 (75.7)
Allo-SCT (%)	299 (14.3)	3 (16.7)	69 (15.1)	88 (14.0)	50 (13.9)	11 (9.2)	78 (15.5)
Hypomethylating agents (%)	340 (16.3)	1 (5.6)	109 (23.8)	149 (23.7)	40 (11.1)	4 (3.4)	37 (7.4)
Best supportive care (%)	298 (14.3)	2 (11.1)	102 (22.3)	96 (15.2)	30 (8.3)	12 (10.1)	56 (11.2)
Other (%)	183 (8.7)	3 (16.7)	55 (12.0)	60 (9.5)	21 (5.8)	15 (12.6)	29 (5.8)

Our data show that AML with an immunophenotypic signature similar to that of HSC (henceforth termed HSC-L) represented 0.9% (Fig. 1C). TUH cohort comprised 21.9% of MPP-L, 30.2% of CMP-L, 17.2% of GMP-L, 24.1% of MP-L, and 5.7% of GP-L. HSC-L and MPP-L were enriched in AML classified as FAB M0, while MP-L was enriched in acute monoblastic leukemia (FAB M5) and GP-L in AML classified as FAB M1 (Fig. 1D). The FAB M6 and M7 represented 2.9% and 1.4% of the TUH cohort, respectively. Classified by phenotype, their SLA were heterogeneous (Fig. 1D). Nevertheless, the SLA of 63.3% of the FAB M6 and M7 was identified as MPP-L or CMP-L, stages prior to the MEP branch (Supplementary Fig. 1A), whereas the remainder

(1.5% of the total cohort) may have been misclassified because of the absence of erythroid and megakaryocytic markers in our panel. Thus, flow-based analysis of SLA correlates with the morphologic phenotype used to assign the FAB sub-group although the correlation is not completely consistent.

SLA retain functional and genetic imprints of their normal counterparts

Following induction of the differentiation process, HSPCs lose their capacity to self-renew, in favor of proliferation and migration. We, therefore, investigated the functional characteristics of the six SLA

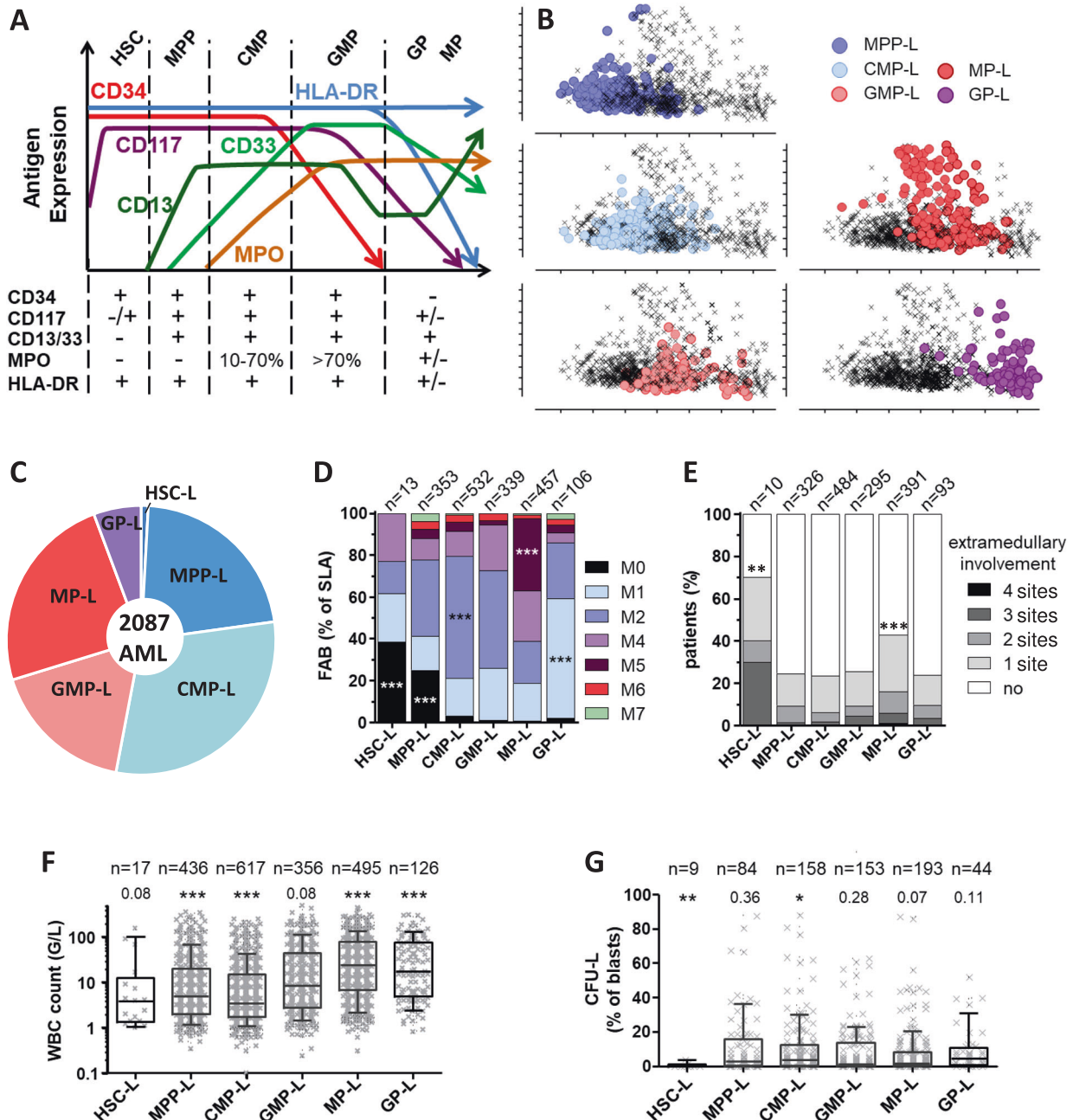


Fig. 1 Phenotypic and clinical identification of AML subgroups. **A** Model of the relative percentage of myeloid marker expression over the course of normal HSPC differentiation. The SLA is defined by the combination of expressions of five myeloid markers plus HLA-DR to differentiate GP-L (HLA-DR+) and MP-L (HLA-DR-); $\geq 20\%$ of blasts; $< 20\%$ of blasts; +/- marker can be positive or negative. **B** Principal component analyses of 945 AML using the percentage of AML blasts expression of 16 markers by flow cytometry (CD4, CD7, CD13, CD33, CD117, MPOc, CD34, HLA-DR, CD56, CD64, CD38, CD65, CD16, CD14, CD11b, CD123). AML patients were classified according to their SLA as detailed in (A). **C** Pie chart of 2087 AML from TUH cohort segregated according to their SLA. **D** FAB classification in one SLA to all others. Fisher's exact test compared FAB classification in one SLA to all others. **E** Extramedullary involvement in SLA (see Table 1 for details). **F** Boxplots of leukocytosis at diagnosis in TUH cohort. **G** CFU-L in TUH cohort. Statistical analysis was performed comparing one SLA to all others (Mann-Whitney test).

using clinical data and clonogenic properties as surrogate markers of migration (extramedullary involvement) and proliferation (leucocytosis) capacities. Cell migration capacities and emigration from the bone marrow are known to be features acquired during differentiation [30]. As a result, the extramedullary disease was significantly more frequently observed in the MP-L group and surprisingly in the low HSC-L group (Fig. 1E). In detail, patients with GMP-L, GP-L, and MP-L displayed a higher rate of lymph node enlargement and leukemic gingival infiltration (Table 1).

However, spleen enlargement was mostly seen in MPP-L. Interestingly, leucocytosis increased as SLA was further advanced in the differentiation process (Fig. 1F and Table 1). Moreover, the clonogenic capacities of the HSC-L, similar to normal HSC [31], were significantly lower than those of other SLA (Fig. 1G).

Since the SLA is defined by HSPCs phenotypes, we hypothesized that the expression of genes known to be expressed in AML could be related to the SLA. To test our hypothesis, we focus on well-described AML prognostic genes *BAALC*, *ERG*, and

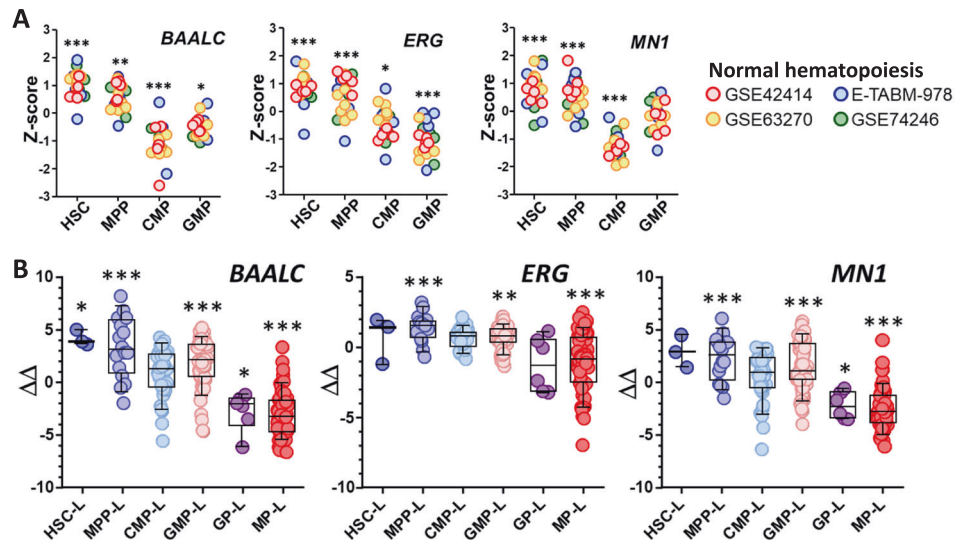


Fig. 2 Genetic validation of SLA classification. **A** Expression of *BAALC*, *ERG*, and *MN1* in four normal HSPCs datasets. Gene expressions were normalized calculating Z-score in each dataset. **B** Expression of *BAALC*, *ERG*, and *MN1* according to SLA subgroups in TUH cohort (fluidigm, $n = 171$).

MN1 [32, 33] and analyzed the publicly available transcriptomic HSPCs database. Those three genes were overexpressed in HSC and their expression level decreased as hematopoietic differentiation progressed (Fig. 2A). Similarly, *BAALC*, *ERG*, and *MN1* were overexpressed in HSC-L and MPP-L and repressed in GP-L and MP-L (Fig. 2B).

Therefore, we showed in the TUH cohort that the different SLAs retained specific biological characteristics of normal hematopoiesis.

SLA correlates with leukemic stem cell profiles of AML

We have previously shown that the level of $CD34^+CD38^-CD123^+$ LSCs is an independent prognostic factor in AML treated with intensive chemotherapy [16, 34]. To study the relationship between SLA and LSC, we measured LSC levels in the TUH cohort (Fig. 3A). HSC-L/MPP-L had the highest levels of $CD34^+CD38^-CD123^+$ LSCs (18.03% vs. 11.54% in CMP-L, 7.83% in GMP-L, <1% in MP-L and GP-L, Kruskal–Wallis test $p < 0.0001$).

To evaluate the stem properties of SLA subsets, we injected leukemic cells from 70 AML in 446 NGS mice (6.4 mice/sample, range 4–20). Early SLA (i.e., MPP-L and CMP-L, 31 AML, 209 mice) had higher number of engrafted mice (64.4% vs. 23.5%, $p = 0.0001$, Fig. 3B), higher levels of engraftment (21.5% vs. 4.7%, $p = 0.0027$, Fig. 3C), and greater expansion of leukemic cells (1.9 vs. 0.2-fold, $p = 0.0002$, Fig. 3D) than late SLA (GMP-L, MP-L, and GP-L, 38 AML, 237 mice).

Together, those data show that stem properties are enriched in early SLA (HSC-L, MPP-L, and CMP-L).

Oncogenic events are specific to SLA

To identify oncogenic events linked to specific SLA, we studied point mutations and cytogenetic anomalies. We screened 46 genes commonly mutated in myeloid malignancies from 409 patients of the TUH cohort and identified 1363 mutations or cytogenetic anomalies (Fig. 4A), with overall frequencies that were consistent with those published in previous studies [35, 36]. We identified at least one driver mutation in 399 patients (97.6%) and two or more driver mutations in 89.7% of the samples.

Although co-mutation or mutual exclusivity profiles have been previously described in AML [35, 36], our cohort allowed a more comprehensive analysis of the driver mutations involved in the maturation block of SLA. We calculated the relative risks (RR) of cytogenetic abnormalities ($n = 1967$, Fig. 4B) and point mutations ($n = 409$, Fig. 4C) for each SLA.

MPP-L and CMP-L show criteria of secondary AML

MPP-L and CMP-L are phenotypically defined as $CD34^+$ AML, positive for myeloid markers ($CD13^+CD33^+CD117^+$); and differ by their expression of cytoplasmic MPO (<10% for MPP-L and within the range of 10–70% for CMP-L). MPP-L and CMP-L show more often cytogenetic abnormalities of AML MRC (Fig. 4B) such as $del(7q)$ (RR:1.85, $p < 0.0001$; RR:1.61, $p < 0.0001$; for MPP-L and CMP-L, respectively), $del(17p)$ (RR:1.77, $p = 0.0010$; RR:1.53, $p = 0.0033$, respectively) and $del(12p)$ (RR:1.63, $p = 0.015$; RR:1.46, $p = 0.021$, respectively). MPP-L and CMP-L are also enriched in secondary AML (s-AML) mutations [37] in normal karyotype ($n = 200$, Supplemental Fig. 3A, B): *ASXL1* (MPP-L RR:6.1; $p = 0.0006$), *SRSF2* (MPP-L RR:5.0; $p = 0.0021$), *EZH2* (MPP-L RR:7.7; $p = 0.024$), *ZRSR2* (MPP-L RR:5.8; $p = 0.046$), *STAG2* (MPP-L RR:2.9; $p = 0.092$), and *SF3B1* (CMP-L RR:3.3; $p = 0.050$), *BCOR* (CMP-L RR:2.7; $p = 0.089$). In order to investigate the relationship between secondary AML and SLA, we rigorously classified 409 AML patients as clinical s-AML (post-MDS or MPN), molecular s-AML (defined as AML with mutations in any of the eight genes frequently altered in MDS [37]) or karyotypic s-AML (Fig. 5). MPP-L and CMP-L were classified s-AML in 68% and 56%, respectively (RR:3.0, $p < 0.0001$). In addition, $inv(3)$ (RR:3.0, $p < 0.0001$), $t(9;22)$ (RR:2.4, $p = 0.0011$), *CSF3R* (normal karyotype RR:12.3, $p < 0.0001$) and *RUNX1* mutations (RR:3.3, $p < 0.0001$) were enriched in MPP-L.

Gene mutations can be further functionally classified into eight categories [35] (Fig. 4D and Supplemental Fig. 3C). MPP-L were enriched in mutations in epigenetic modifiers (RR: 2.1, $p = 0.001$), spliceosome (RR:1.9, $p = 0.01$) and myeloid transcription factors (mainly *RUNX1* and *ETV6* mutations, RR:1.9, $p = 0.008$).

Bi-allelic CEBPA mutations and CBF abnormalities are specific of GMP-L

GMP-L is defined with a classic phenotype $CD34^+CD13^+CD33^+CD117^+$ and high expression of cytoplasmic MPO (>70%). Astonishingly, it was very specific of three abnormalities (Fig. 4B, C): $inv(16)$ (RR:5.6, $p < 0.0001$), $t(8;21)$ (RR:5.2, $p < 0.0001$) and *CEBPA* mutations (RR:4.8, $p < 0.0001$). We further studied *CEBPA* mutations in 871 AML from the TUH cohort and found the mutation in 35.7% of GMP-L (46/129, RR:6.2, $p < 0.0001$, Supplemental Fig. 4A), the majority of which were bi-allelic mutations (72%, 33/46). Overall, CBF abnormalities represented 33% of GMP-L (119/360 patients).

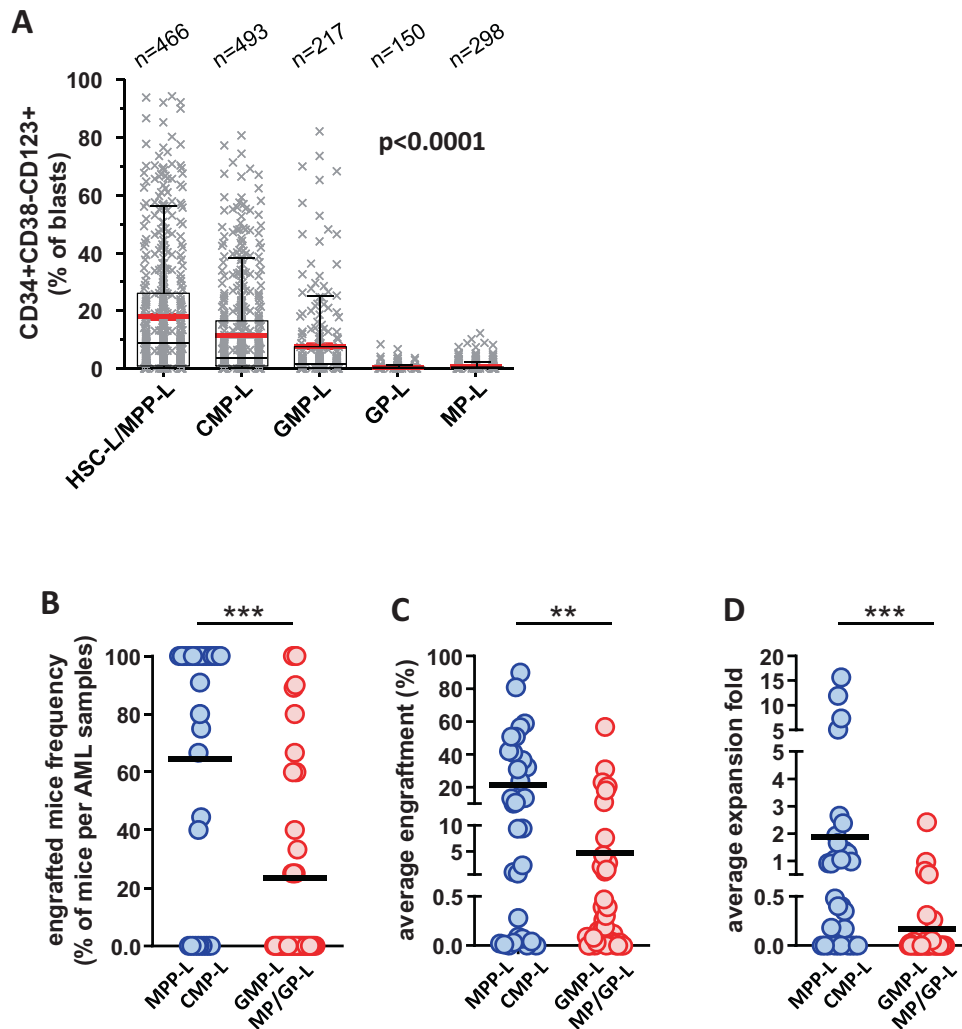


Fig. 3 Stem cell properties are related to the SLA. **A** Percentage of leukemic stem cells ($CD34^+CD38^-CD123^+$) among blasts according to SLA in the TUH cohort (Kruskal–Wallis test). **B–D** Patient-derived xenograft from 70 AML patient samples in 446 mice. A group of five mice is classically used to test an AML sample with an injected dose of 10^7 cells per mouse. Engraftment is assessed in a delay of 16 weeks. **B** Percentage of mice with $>0.5\%$ of human leukemic cells detected in bone marrow samples by flow cytometry. **C** Evaluation of human leukemic engraftment in bone marrow samples of each experiment. Each point represents the mean of all PDX of a donor. **D** Expansion fold is calculated as a ratio between engrafted cells in mice bone marrow and spleen and injected leukemic cells.

MP-L and GP-L are the two sides of *NPM1* mutated AML

MP-L and GP-L are phenotypically defined as $CD34^-$ AML, positive for myeloid markers ($CD13^+CD33^+CD117^{+/-}$); and differ by their expression of HLA-DR ($\geq 20\%$ for MP-L and $< 20\%$ for GP-L). Both groups frequently expressed *NPM1* mutation (MP-L RR:3.8, $p < 0.0001$; GP-L RR:6.0, $p < 0.0001$, Fig. 4C). However, *NPM1* mutations were associated with mutations of *DNMT3A* (RR:2.3, $p < 0.0001$) and *FLT3* (RR:2.1, $p < 0.0001$) in MP-L, and with *TET2* mutations in GP-L, (RR:4.6, $p < 0.0001$). Mutations in *TET2*, *IDH1*, and *IDH2* are largely mutually exclusive and lead to similar epigenetic changes [38]. Since the *TET2* mutations were enriched in GP-L, we looked at the distribution of *IDH1* and *IDH2* mutations in the TUH cohort and found that these mutations were also enriched in GP-L (Supplemental Fig. 4B). Indeed, the GP-L subgroup was composed of *NPM1/TET2* mutated and *NPM1/IDH1* or *NPM1/IDH2* mutated patients (52% and 20% of GP-L, respectively). Of note, besides the *NPM1*-mutated MP-L subset which accounts for 64% of all MP-L and 82% of normal karyotype MP-L, *MLL* fusions were enriched in this SLA (RR:2.4, $p < 0.0001$; Fig. 4B) although their frequency is modest (59 patients in TUH cohort including 32 MP-L).

SLA correlates by chemoresistance and outcome of patients treated by intensive chemotherapy

We investigated ex-vivo chemosensitivity and the response to intensive chemotherapy of AML patients according to their SLA. Ex-vivo apoptosis testing of 47 AML samples incubated with cytarabine (AraC) showed that MPP-L and CMP-L had a significantly higher IC_{50} than GMP-L and GP/MP-L (>1000 vs. 540 and 33 μM , respectively, Fig. 6A). Moreover, AML patients with immature SLA had a higher percentage of residual blasts in bone marrow at day 15 after intensive chemotherapy (Fig. 6B) and consequently, a lower complete response rate than patients with more mature SLA (HSC/MPP-L 72%; CMP-L 76%; GMP-L 87%; MP-L 85%; GP-L 79%; $p < 0.0001$). As a result, overall survival was significantly worse in patients with immature compared to mature SLA ($p < 0.0001$, Fig. 6C and Supplemental Fig. 5A) even though the early death rate was higher in hyperleukocytic SLA (GP-L and MP-L, Table S2). The cumulative incidence of relapse (CIR) was also significantly higher in the immature SLA group ($p < 0.0001$, Fig. 6D and Supplemental Fig. 6A). The correlation between SLA and response to chemotherapy was confirmed in younger AML patients (Supplemental Figs. 5B and 6B). Consistent with their

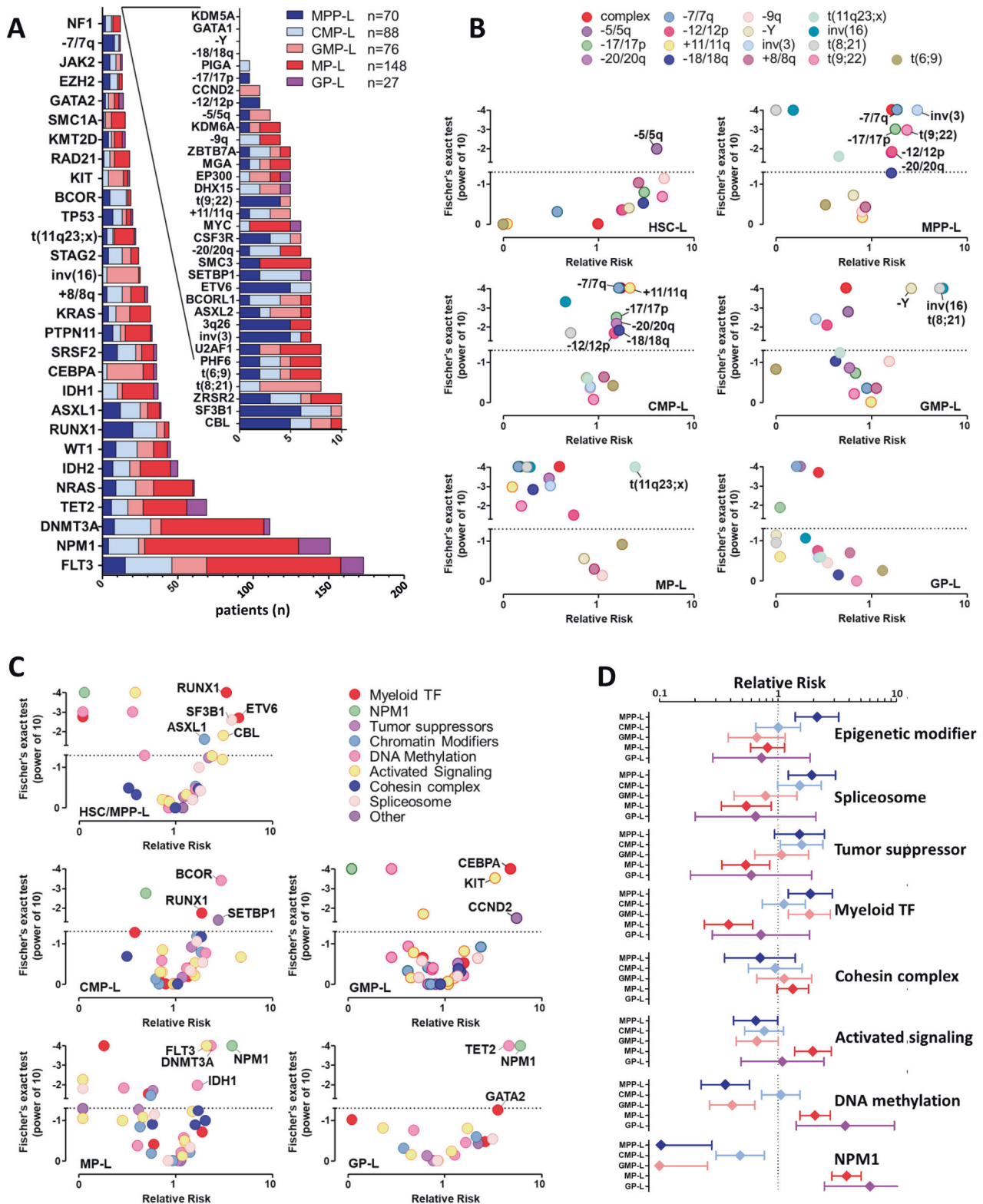


Fig. 4 Distribution of AML mutations and genetic abnormalities according to the SLA. **A** Number of patients with specific mutations or genetic abnormalities ($n = 409$). **B** Volcano plots of relative risk of the presence of specific genetic anomalies in each SLA ($n = 1967$). **C** Volcano plots of relative risk of the presence of specific mutations in each SLA ($n = 409$). **D** Plots of relative risks of eight functional modules of mutations [35] in SLA.

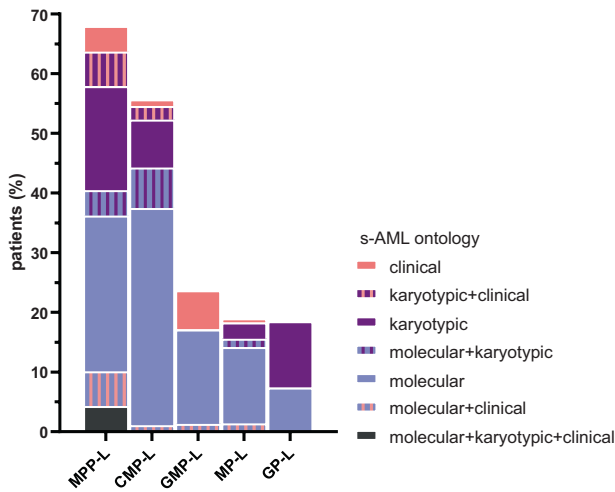


Fig. 5 Secondary AML according to the SLA. Definition of secondary AML in 409 patients based on an association of clinical (history of MDS or MPN), molecular (mutations in any of the eight genes frequently altered in MDS [37]) and/or karyotypic abnormalities as defined by WHO.

chemoresistance status, allogeneic stem cell transplant in first complete remission was of great survival benefit for MPP-L and CMP-L and showed little or no survival improvement in the other groups (Table S3). Interestingly, SLA of relapsed AML ($n = 193$) was identical or more immature to diagnostic, in most of the cases (57% and 27%, respectively, Table S4). When a more mature SLA was identified at relapse (16%, 30/193), we observed, when available, a modification of the mutational profile in half of the cases (8/16).

In multivariate models, SLA classification retained independent prognostic values for overall survival, event-free survival, and cumulative incidence of relapse (Tables S5 and S6). Of note, GP-L represented a good prognostic subgroup, with a plateau of CIR at 37% in the TUH cohort (Supplemental Fig. 6A) and 19% in those under 60 (Supplemental Fig. 6B).

Altogether, these data indicate that the chemoresistance of AML cells is, at least in part, a consequence of innate (SLA imprint) and acquired (oncogenic events) mechanisms (see Table S7 for the summary of characteristics of SLA).

Validation in an independent cohort of 1209 AML patients

To robustly validate our signatures, we took advantage of a second AML cohort: 1209 patients diagnosed at Bordeaux University Hospital (BUH cohort, see Table S1). Similarly, to the TUH cohort, the BUH cohort comprised 0.7% of HSC-L, 11.7% of MPP-L, 27.9% of CMP-L, 28.4% of GMP-L, 21.9% of MP-L, and 9.4% of GP-L (Supplemental Fig. 7A). HSC-L and MPP-L were enriched in AML classified as FAB M0, while MP-L were enriched in acute monoblastic leukemia (FAB M5) and GP-L in AML classified as FAB M1 (Supplemental Fig. 7B). Leukocytosis increased as SLA was further advanced in the differentiation process (Supplemental Fig. 7C).

In the BUH cohort, we found that *inv(3)* (Supplemental Fig. 8A) were enriched in MPP-L, whereas *ASXL1* mutation and *t(9;22)* were increased but not statistically specific to this SLA (Supplemental Fig. 8B, C); *inv(16)*, *t(8;21)* and bi-allelic *CEBPA* mutations were enriched in GMP-L (Supplemental Fig. 8D, E); *MLL* fusions and *NPM1* and *DNMT3A* mutations were enriched in MP-L (Supplemental Fig. 8F–H) whereas *NPM1* and *TET2* and *IDH* mutations were enriched in GP-L (Supplemental Fig. 8I–K).

In the BUH cohort, SLA retained their prognostic factor, with increased D15 blasts (Supplemental Fig. 9A), and worse OS and CIR (Supplemental Fig. 9B, C) in immature SLA.

DISCUSSION

It has long been possible to immunophenotypically classify acute lymphoblastic leukemia [39–41]. These classifications are based on the expression by normal lymphocytes of antigens that are specific for different maturation stages. To date, such classifications do not apply to leukemia of the myeloid lineage likely because human myelopoiesis is less strictly defined than lymphopoiesis and is regularly reconsidered [3, 4, 12, 42–45]. Here, we presented a phenogenomic framework of AML that provides insight into the pathogenesis of AML and that identifies molecular features influencing therapy response. We discovered five distinct phenotypic subgroups that differ by specific surface protein expression patterns and hence provide a phenotypic classification of AML. Our study builds on previous work that cataloged genetic aberrations in AML and linked them to clinical outcomes, resulting in a genomic classification of the disease [36, 46]. We showed an exclusive association between a few genomic alterations and hematopoietic maturation stages. Interestingly, previous transcriptomic studies found at least 16 AML subgroups that were also associated with specific cytogenetic features and mutations [47]. Of these, only the GMP-L-associated genomic aberrations (*CEBPAm*, *t(8;21)* and *inv16*) were directly associated with transcriptomic clusters. Altogether, this suggests that, in most cases, genomic, transcriptomic, and proteomic data are independent and complementary.

The clinical relevance of our AML proteomic classification is further supported by the fact that proteomic clusters significantly differed in their outcomes in patients treated with intensive chemotherapy. Moreover, complementary to morphological analysis, we believe that this classification which can be available on the day of diagnosis, whereas cytogenetic and molecular abnormalities are available only a few days later or sometimes missing, may inform physicians on the disease subtype and contribute to patient management (Supplemental Fig. 10).

Although the SLA classification clearly segregated HSC-L/MPP-L from GMP-L and GP-L/MP-L, the CMP-L subgroup was more heterogeneous. This may suggest that this stage is insufficiently characterized by its immunophenotypic signature and/or that its normal counterpart is itself heterogeneous and should be separated into several more homogeneous stages. Alternately, complex mechanisms of differentiation arrest could apply to this subtype in which no recurrent genetic events were identified at variance with HSC-L, MPP-L, GMP-L, GP-L, and MP-L. More studies are needed to identify new surface markers in order to refine the SLA classification which may encompass more groups.

Our findings also suggest that few oncogenic events may be responsible for the SLA. *RUNX1* mutations and *inv(3)* are associated with MPP-L, abnormalities of secondary AML with MPP-L and CMP-L, *CEBPA* mutations, *RUNX1-RUNX1T1* or *CBFB-MYH11* translocations with GMP-L, *NPM1*, and *TET2* or *IDH* mutations with GP-L and *NPM1* and *DNMT3A* mutations and *t(11q23)* with MP-L. As noted, future studies will need to further clarify the genotype–phenotype correlations of AML as improved myeloid maturation markers are developed.

The subclonal architecture of AML has been already described [48]. Hypothetically, the presence of different leukemic clones, blocked at different stages, could interfere with the SLA signature determination. Although we cannot completely exclude this possibility, some elements argue in favor of a weak impact of subclonal architecture on SLA signatures: (i) most AML at the time of diagnosis are composed of a major founding clone likely to be detected by the SLA signature [35, 48]; (ii) oncogenic mutations strongly linked to SLA are rarely found in pre-leukemic clones (except *DNMT3A* or *TET2* mutations) but are likely a later event in leukemogenesis [49, 50]; and consequently (iii) these oncogenic events are mutually exclusive and rarely found associated in AML patients. Nevertheless, the molecular complexity of CMP-L raises the question of the subclonal architecture of this subtype. Further

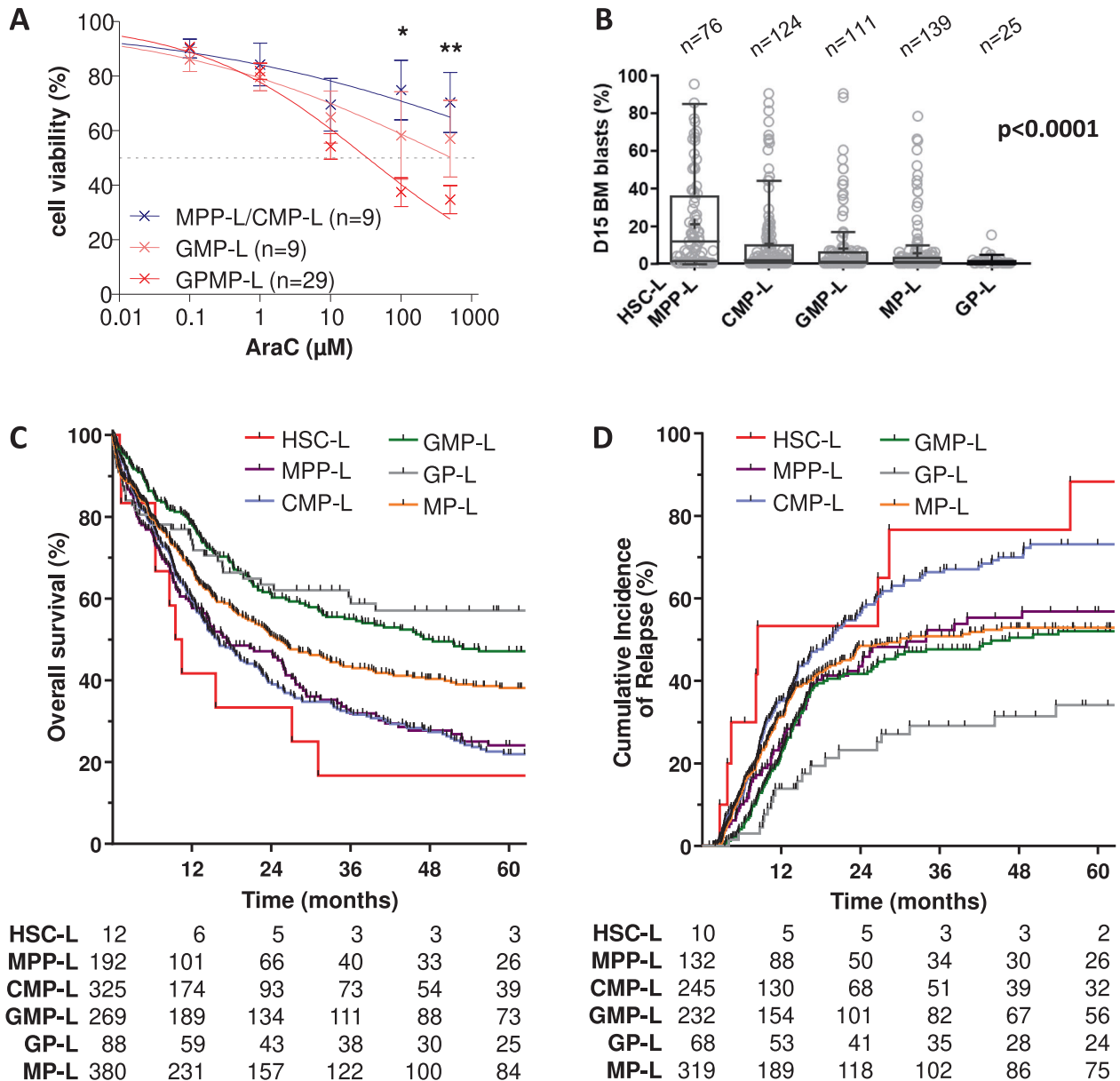


Fig. 6 Response to chemotherapy according to the SLA. **A** In vitro testing of cytarabine (AraC) activity in 47 AML samples. **B** Early chemosensitivity according to SLA was evaluated in patients by measuring the percentage of residual blasts in bone marrow at day 15 of induction chemotherapy ($n = 475$). **C** Prognostic impact of SLA on overall survival for patients from TUH cohort treated with intensive chemotherapy ($n = 1266$). See Table S2 for multivariate analysis results. **D** Prognostic impact of SLA on overall survival for younger patients (< 60 years) from TUH cohort treated with intensive chemotherapy ($n = 638$).

genetic and immunophenotypic studies are needed to fully explore the relationship between SLA and AML architecture as some leukemic clones show functional heterogeneity [51].

In vitro studies of chemosensitivity and clinical data also demonstrated that the SLA classification could predict response to the main therapeutic strategy used in AML. Indeed, GMP-L/GP-L/MP-L encompass the more chemosensitive genetic subgroups (i.e., *RUNX1-RUNX1T1*, *CBFB-MYH11*, *CEBPA*, and *NPM1* mutations) do benefit from intensive chemotherapy as compared with HSC-L/MPP-L/CMP-L. Obviously, it will be very interesting to describe the impact of new therapeutic combinations such as azacitidine and venetoclax in this context [52]. Furthermore, this SLA classification is a useful tool in clinical practice because it may predict on the day of diagnosis in which genetic subgroup patients will be ultimately classified by chromosomal and

molecular analyses. This may have an impact on clinical management. Furthermore, this correlation may suggest that AMLs that are more closely related to HSPC are most likely to retain the chemoresistance properties of HSCs. Studies of the phenotype of residual leukemic cells after chemotherapy induction may help clarify the biology of chemoresistance.

In summary, AML immunophenotyping can establish a new SLA classification that strongly correlates with cellular behavior of the leukemic bulk, and predicts main genetic subgroups early at diagnosis and outcome after intensive chemotherapy. Each SLA is defined by specific oncogenic events whose penetrance may be dependent on the differentiation stages of hematopoiesis and their gene expression. Identifying disrupted gene pathways specific for each SLA should therefore form the basis for targeted therapies aimed at inducing AML differentiation.

DATA AVAILABILITY

The datasets generated during and/or analyzed during the current study are available from the corresponding authors on reasonable request.

REFERENCES

- Murray L, Chen B, Galy A, Chen S, Tushinski R, Uchida N, et al. Enrichment of human hematopoietic stem cell activity in the CD34+Thy-1+Lin- subpopulation from mobilized peripheral blood. *Blood* 1995;85:368–78.
- Ishikawa F, Yasukawa M, Lyons B, Yoshida S, Miyamoto T, Yoshimoto G, et al. Development of functional human blood and immune systems in NOD/SCID/IL2 receptor [gamma] chain(null) mice. *Blood* 2005;106:1565–73.
- Majeti R, Park CY, Weissman IL. Identification of a hierarchy of multipotent hematopoietic progenitors in human cord blood. *Cell Stem Cell*. 2007;1:635–45.
- Doulatov S, Notta F, Eppert K, Nguyen LT, Ohashi PS, Dick JE. Revised map of the human progenitor hierarchy shows the origin of macrophages and dendritic cells in early lymphoid development. *Nat Immunol*. 2010;11:585–93.
- Akashi K, Traver D, Miyamoto T, Weissman IL. A clonogenic common myeloid progenitor that gives rise to all myeloid lineages. *Nature* 2000;404:193–7.
- Kondo M, Weissman IL, Akashi K. Identification of clonogenic common lymphoid progenitors in mouse bone marrow. *Cell* 1997;91:661–72.
- Meyer SC, Levine RL. Translational implications of somatic genomics in acute myeloid leukaemia. *Lancet Oncol*. 2014;15:e382–94.
- Genovese G, Kahler AK, Handsaker RE, Lindberg J, Rose SA, Bakhoum SF, et al. Clonal hematopoiesis and blood-cancer risk inferred from blood DNA sequence. *N Engl J Med*. 2014;371:2477–87.
- Jaiswal S, Fontanillas P, Flannick J, Manning A, Grauman PV, Mar BG, et al. Age-related clonal hematopoiesis associated with adverse outcomes. *N Engl J Med*. 2014;371:2488–98.
- Bonnet D, Dick JE. Human acute myeloid leukemia is organized as a hierarchy that originates from a primitive hematopoietic cell. *Nat Med*. 1997;3:730–7.
- Sarry JE, Murphy K, Perry R, Sanchez PV, Secretro A, Keefer C, et al. Human acute myelogenous leukemia stem cells are rare and heterogeneous when assayed in NOD/SCID/IL2Rgammac-deficient mice. *J Clin Invest*. 2011;121:384–95.
- Goardon N, Marchi E, Atzberger A, Quek L, Schuh A, Soneji S, et al. Coexistence of LMPP-like and GMP-like leukemia stem cells in acute myeloid leukemia. *Cancer Cell*. 2011;19:138–52.
- Bhatt S, Pioso MS, Olesinski EA, Yilma B, Ryan JA, Mashaka T, et al. Reduced mitochondrial apoptotic priming drives resistance to BH3 mimetics in acute myeloid leukemia. *Cancer Cell*. 2020;38:872–90.e6.
- Chopra S, Ramkissoon K, Anderson DC. A systematic quantitative proteomic examination of multidrug resistance in *Acinetobacter baumannii*. *J Proteom*. 2013;84:17–39.
- Hu Z, Yuan J, Long M, Jiang J, Zhang Y, Zhang T, et al. The Cancer Surfaceome Atlas integrates genomic, functional and drug response data to identify actionable targets. *Nat Cancer* 2021;2:1406–22.
- Vergez F, Green AS, Tamburini J, Sarry JE, Gaillard B, Cornillet-Lefebvre P, et al. High levels of CD34+CD38low/-CD123+ blasts are predictive of an adverse outcome in acute myeloid leukemia: a Groupe Ouest-Est des Leucemies Aigues et Maladies du Sang (GOELAMS) study. *Haematologica* 2011;96:1792–8.
- Dufva O, Polonen P, Bruck O, Keranen MAI, Klievink J, Mehtonen J, et al. Immunogenomic landscape of hematological malignancies. *Cancer Cell*. 2020;38:424–8.
- Jayavelu AK, Wolf S, Buettner F, Alexe G, Haupt B, Comoglio F, et al. The proteogenomic subtypes of acute myeloid leukemia. *Cancer Cell*. 2022;40:301–17.e12.
- LaRochelle O, Bertoli S, Vergez F, Sarry JE, Mansat-De Mas V, Dobbstein S, et al. Do AML patients with DNMT3A exon 23 mutations benefit from idarubicin as compared to daunorubicin? A single center experience. *Oncotarget* 2011;2:850–61.
- Bertoli S, Berard E, Huguet F, Huynh A, Tavitian S, Vergez F, et al. Time from diagnosis to intensive chemotherapy initiation does not adversely impact the outcome of patients with acute myeloid leukemia. *Blood* 2013;121:2618–26.
- Bertoli S, Dumas PY, Berard E, Largeaud L, Bidet A, Delabesse E, et al. Outcome of relapsed or refractory FLT3-mutated acute myeloid leukemia before second-generation FLT3 tyrosine kinase inhibitors: a Toulouse-Bordeaux DATAML Registry Study. *Cancers (Basel)*. 2020;12:773.
- Dumas PY, Bertoli S, Berard E, Largeaud L, Bidet A, Delabesse E, et al. Real-world outcomes of patients with refractory or relapsed FLT3-ITD acute myeloid leukemia: a Toulouse-Bordeaux DATAML Registry Study. *Cancers (Basel)*. 2020;12:2044.
- Pabst T, Mueller BU, Zhang P, Radomska HS, Narravula S, Schnittger S, et al. Dominant-negative mutations of CEBPA, encoding CCAAT/enhancer binding protein-alpha (C/EBPalpha), in acute myeloid leukemia. *Nat Genet*. 2001;27:263–70.
- McKenna A, Hanna M, Banks E, Sivachenko A, Cibulskis K, Kernytzky A, et al. The Genome Analysis Toolkit: a MapReduce framework for analyzing next-generation DNA sequencing data. *Genome Res*. 2010;20:1297–303.
- Poplin R, Ruano-Rubio V, DePristo MA, Fennell TJ, Carneiro MO, Van der Auwera GA, et al. Scaling accurate genetic variant discovery to tens of thousands of samples [Preprint]. 2018. Available from: <https://doi.org/10.1101/201178>.
- Laurenti E, Doulatov S, Zandi S, Plumb I, Chen J, April C, et al. The transcriptional architecture of early human hematopoiesis identifies multilevel control of lymphoid commitment. *Nat Immunol*. 2013;14:756–63.
- Corces MR, Buenostro JD, Wu B, Greenside PG, Chan SM, Koenig JL, et al. Lineage-specific and single-cell chromatin accessibility charts human hematopoiesis and leukemia evolution. *Nat Genet*. 2016;48:1193–203.
- Jung N, Dai B, Gentles AJ, Majeti R, Feinberg AP. An LSC epigenetic signature is largely mutation independent and implicates the HOXA cluster in AML pathogenesis. *Nat Commun*. 2015;6:8489.
- Cheson BD, Bennett JM, Kopecky KJ, Buchner T, Willman CL, Estey EH, et al. Revised recommendations of the International Working Group for diagnosis, standardization of response criteria, treatment outcomes, and reporting standards for therapeutic trials in acute myeloid leukemia. *J Clin Oncol*. 2003;21:4642–9.
- Mohle R, Moore MA, Nachman RL, Rafii S. Transendothelial migration of CD34+ and mature hematopoietic cells: an in vitro study using a human bone marrow endothelial cell line. *Blood* 1997;89:72–80.
- Petzer AL, Hogge DE, Landsdorp PM, Reid DS, Eaves CJ. Self-renewal of primitive human hematopoietic cells (long-term-culture-initiating cells) in vitro and their expansion in defined medium. *Proc Natl Acad Sci USA*. 1996;93:1470–4.
- Haferlach C, Kern W, Schindela S, Kohlmann A, Alpermann T, Schnittger S, et al. Gene expression of BAALC, CDKN1B, ERG, and MN1 adds independent prognostic information to cytogenetics and molecular mutations in adult acute myeloid leukemia. *Genes Chromosomes Cancer*. 2012;51:257–65.
- Metzeler KH, Dufour A, Benthaus T, Hummel M, Sauerland MC, Heinecke A, et al. ERG expression is an independent prognostic factor and allows refined risk stratification in cytogenetically normal acute myeloid leukemia: a comprehensive analysis of ERG, MN1, and BAALC transcript levels using oligonucleotide microarrays. *J Clin Oncol*. 2009;27:5031–8.
- Vergez F, Nicolau-Travers ML, Bertoli S, Rieu JB, Tavitian S, Bories P, et al. CD34(+) CD38(-)CD123(+) leukemic stem cell frequency predicts outcome in older acute myeloid leukemia patients treated by intensive chemotherapy but not hypomethylating agents. *Cancers (Basel)*. 2020;12:1174.
- TCGA_network. Genomic and epigenomic landscapes of adult de novo acute myeloid leukemia. *N Engl J Med*. 2013;368:2059–74.
- Papaemmanuil E, Gerstung M, Bullinger L, Gaidzik VI, Paschka P, Roberts ND, et al. Genomic classification and prognosis in acute myeloid leukemia. *N Engl J Med*. 2016;374:2209–21.
- Lindsley RC, Mar BG, Mazzola E, Grauman PV, Shareef S, Allen SL, et al. Acute myeloid leukemia ontogeny is defined by distinct somatic mutations. *Blood* 2015;125:1367–76.
- Figuerola ME, Abdel-Wahab O, Lu C, Ward PS, Patel J, Shih A, et al. Leukemic IDH1 and IDH2 mutations result in a hypermethylation phenotype, disrupt TET2 function, and impair hematopoietic differentiation. *Cancer Cell*. 2010;18:553–67.
- Greaves MF. Differentiation-linked leukemogenesis in lymphocytes. *Science* 1986;234:697–704.
- Nadler LM, Korsmeyer SJ, Anderson KC, Boyd AW, Slaughenhoupt B, Park E, et al. B cell origin of non-T cell acute lymphoblastic leukemia. A model for discrete stages of neoplastic and normal pre-B cell differentiation. *J Clin Invest*. 1984;74:332–40.
- Bene MC, Castoldi G, Knapp W, Ludwig WD, Matutes E, Orfao A, et al. Proposals for the immunological classification of acute leukemias. European Group for the Immunological Characterization of Leukemias (EIGL). *Leukemia* 1995;9:1783–6.
- Gorgens A, Radtke S, Mollmann M, Cross M, Durig J, Horn PA, et al. Revision of the human hematopoietic tree: granulocyte subtypes derive from distinct hematopoietic lineages. *Cell Rep*. 2013;3:1539–52.
- Mori Y, Chen JY, Pluvinage JV, Seitza J, Weissman IL. Prospective isolation of human erythroid lineage-committed progenitors. *Proc Natl Acad Sci USA*. 2015;112:9638–43.
- Notta F, Zandi S, Takayama N, Dobson S, Gan OI, Wilson G, et al. Distinct routes of lineage development reshape the human blood hierarchy across ontogeny. *Science*. 2016;351:aab2116.
- Velten L, Haas SF, Blaszkiewicz S, Islam S, Hennig BP, et al. Human hematopoietic stem cell lineage commitment is a continuous process. *Nat Cell Biol*. 2017;19:271–81.
- Dohner H, Estey E, Grimwade D, Amadori S, Appelbaum FR, Buchner T, et al. Diagnosis and management of AML in adults: 2017 ELN recommendations from an international expert panel. *Blood* 2017;129:424–47.
- Valk PJ, Verhaak RG, Beijnen MA, Erpelinck CA, Barjesteh van Waalwijk van Doorn-Khosrovani S, Boer JM, et al. Prognostically useful gene-expression profiles in acute myeloid leukemia. *N Engl J Med*. 2004;350:1617–28.

48. Welch JS, Ley TJ, Link DC, Miller CA, Larson DE, Koboldt DC, et al. The origin and evolution of mutations in acute myeloid leukemia. *Cell* 2012;150:264–78.
49. Engle EK, Fisher DA, Miller CA, McLellan MD, Fulton RS, Moore DM, et al. Clonal evolution revealed by whole genome sequencing in a case of primary myelofibrosis transformed to secondary acute myeloid leukemia. *Leukemia* 2015;29:869–76.
50. Corces-Zimmerman MR, Hong WJ, Weissman IL, Medeiros BC, Majeti R. Pre-leukemic mutations in human acute myeloid leukemia affect epigenetic regulators and persist in remission. *Proc Natl Acad Sci USA*. 2014;111:2548–53.
51. Klcó JM, Spencer DH, Miller CA, Griffith M, Lamprecht TL, O’Laughlin M, et al. Functional heterogeneity of genetically defined subclones in acute myeloid leukemia. *Cancer Cell*. 2014;25:379–92.
52. DiNardo CD, Wei AH. How I treat acute myeloid leukemia in the era of new drugs. *Blood* 2020;135:85–96.

ACKNOWLEDGEMENTS

The authors thank all the members of the G.A.E.L. (*Gaël Adolescent Espoir Leucémie*) association and the members of the Stem Cell and Xenograft Core at the University of Pennsylvania (Philadelphia, PA). This work has been granted by the French government under the «*Investissement d’avenir*» program (ANR-11-PHUC-001), the Institut National du Cancer (INCA-PLBIO 2012-105), the *InnaBioSanté* foundation (RESISTAML project), the *Ligue Contre le Cancer* and the “*Groupement Interrégional de Recherche Clinique et d’Innovation Sud-Ouest Outre-Mer*” (AML StemFlow project). We thank Dr. Marie Christine Béné, Dr. Mary Selak, and Dr. Martin Carroll for the critical reading of the article. We are also grateful to Mr. Jean Delpouy, his family, and friends for their generous support.

AUTHOR CONTRIBUTIONS

Conceptualization, FV; Methodology, FV, LL, JES, and CR; Investigation, FV, LL, SB, M-LNT, AFV, J-BR, IV, ES, AS, ST, FH, JPV, NL, AB, P-YD, AP, IL, VM-D, ED, MC, GD-D, and CR; Writing—original draft, FV and CR; Writing—review & editing, FV, J-ES, MC, GD-D, and CR; Funding acquisition, FV, J-ES, and CR, Supervision, CR.

COMPETING INTERESTS

The authors declare no competing interests.

ADDITIONAL INFORMATION

Supplementary information The online version contains supplementary material available at <https://doi.org/10.1038/s41408-022-00712-7>.

Correspondence and requests for materials should be addressed to François Vergez or Christian Récher.

Reprints and permission information is available at <http://www.nature.com/reprints>

Publisher’s note Springer Nature remains neutral with regard to jurisdictional claims in published maps and institutional affiliations.



Open Access This article is licensed under a Creative Commons Attribution 4.0 International License, which permits use, sharing, adaptation, distribution and reproduction in any medium or format, as long as you give appropriate credit to the original author(s) and the source, provide a link to the Creative Commons license, and indicate if changes were made. The images or other third party material in this article are included in the article’s Creative Commons license, unless indicated otherwise in a credit line to the material. If material is not included in the article’s Creative Commons license and your intended use is not permitted by statutory regulation or exceeds the permitted use, you will need to obtain permission directly from the copyright holder. To view a copy of this license, visit <http://creativecommons.org/licenses/by/4.0/>.

© The Author(s) 2022